On the Optimisation of a Noncoherent CDMA System Based on M-ary Orthogonal Modulation

M. Benthin, K.D. Kammeyer, R. Mann Pelz, and D. Nikolai

Abstract. This paper concerns the optimisation of a DS-CDMA based mobile communication system with respect to the transmission quality in the case of data and video services respectively. For combatting transmission errors, forward error protection based on convolutional codes and interleaving in connection with soft decision maximum-likelihood (ML) decoding through the Viterbi algorithm is applied. In this context, a technique to generate post-decision reliability information in the case of a noncoherent DS-CDMA receiver for a given ML metric is presented. The proposed error control strategy involves the application of equal error protection for raw data transmission with the average post-decoding BER as an optimisation criterion. In the case of a video transmission, a-priori knowledge regarding the error sensitivity of individual parameter sets suggests an unequal error protection strategy based on punctured convolutional codes, where the segmental SNR at the source codec output represents the optimisation criterion. Due to the high complexity of the system under investigation, corresponding results are obtained through simulation of the point-to-point transmission link. A significant gain regarding the achievable transmission quality with respect to conventional approaches can be achieved in connection with a compound design of source coding, channel coding and spectral spreading.

1 Introduction

For the design of efficient mobile radio communication systems, much attention has been paid to code division multiple access (CDMA) in recent years. One of the most popular proposals is the well-known QUALCOMM system [1, 2, 3] recently defined as the IS-95 standard for cellular mobile telephony [4].

Usually, for the uplink and the downlink different concepts are applied due to the different channel conditions. In the downlink, synchronous CDMA in connection with coherent receivers can easily be realised: since each of the mobile users receives all signals transmitted by the base station via identical channel characteristics, one of these signals can be provided with specific training information in order to facilitate the channel estimation. In contrast, in the uplink the problem of channel estimation is much more complicated due to the different locations of the transmitting mobile stations. For this reason, coherent direct sequence (DS) CDMA concepts recently proposed make use of user-specific control channels to obtain estimates of the individual uplink characteristics (e.g. physical control channel (PCCH) in the CODIT ([1])-uplink,[5]). On the other hand, noncoherent uplink concepts have been considered which do not need channel estimation at all. The most famous approach is the QUALCOMM uplink system which is based on a specific form of *M-ary orthogonal modulation*. A detailed comparison of the QUALCOMM and the CODIT system is presented in [6]. In the next section, a short review of the QUALCOMM uplink concept will be given.

Efficient channel coding is required in a mobile radio environment in order to obtain suitable bit error rates (BER). Optimum decoding, e.g. of a convolutional code, is performed by the application of a soft input Viterbi algorithm (VA) where channel state information is exploited [7]. The calculation of bit-specific reliability information for the case of M-ary modulation is not trivial. A ML criterion recently proposed in [9] will be discussed in section 2.2 in more detail for a noncoherent RAKE receiver in "square-law combining" structure.

Applying CDMA techniques for multiuser separation, the bit error probability can be decreased by means of powerful codes, e.g. convolutional codes with code rate R, without further bandwidth expansion. Here, the bandwidth remains unchanged due to the exploitation of the inherently available overall spreading factor ("processing gain", P_G). Another way of decreasing the bit error probability is to share the processing gain between a channel coding and the M-ary orthogonal Walsh modulation described in section 2.1. In this case and for a fixed processing gain, the system performance depends on the specific choice of the parameters R and M. In [10], investigations on the optimum trade-off between code rate and spreading are presented for the special case of 64-ary orthogonal modulation, where $M = 64$ corresponds to the QUALCOMM proposal. In section 3 of this paper, the parameter M will be included in the optimisation procedure. Furthermore, it will be shown that system performance depends on a proper design of the interleaver – it will be demonstrated that a lower code rate will not necessarily result in a lower BER if the delay caused by the interleaver is fixed. The optimisation carried out in section 3 results in the minimum BER and can be regarded as an optimum design if data transmission is applied.

In the case of an audio and/or video transmission, the average BER does not necessarily

[1] **Co**de **Di**vision **T**estbed, European RACE program

represent the proper performance criterion. This is due to the fact that individual parameter sets (e.g. parametric source coding), subsequences (e.g. hierarchical source coding) or objects (e.g. object-oriented source coding) of the source coded audio/video sequences are characterised by different information contents which exhibit unequal sensitivity to transmission errors. Error control strategies which make use of this a-priori knowledge in the case of a speech and video transmission in dedicated mobile environments were proposed in [17] and [18]. A similar approach is sought for low data rate video transmission in the considered DS-CDMA based mobile system. The corresponding error control strategy proposed in section 4 is characterised by selective error protection of individual parameter sets by application of punctured convolutional codes in conjunction with soft decision decoding based on the ML metric to be derived in section 2.2. A key issue is the optimum choice of key design parameters such as source accuracy, redundancy and spectral spreading. Corresponding results which are obtained by a discrete optimisation process based on the simulation of the point-to-point transmission system are presented. As an objective performance measure, the segmental SNR at the output of the video source codec is applied.

2 DS-CDMA with ML Soft Decision Channel Decoding

2.1 M-ary Orthogonal Modulation Technique

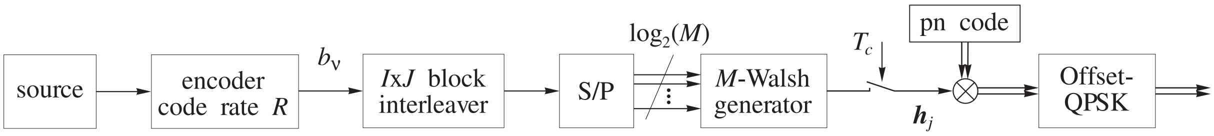

Fig. 1: CDMA transmitter with orthogonal modulation.

Fig. 1 shows the fundamental block diagramm of the transmitter. After channel encoding (code rate R) and interleaving, bit groups of length $\log_2(M)$ are mapped onto a set of M real-valued symbols ([2]) $\boldsymbol{h}_j$, $j \in \{0, \ldots, M-1\}$. If the symbols are orthogonal, i.e. $\boldsymbol{h}_i^T \boldsymbol{h}_j = 0$, $i \neq j$, this mapping procedure can be interpreted as orthogonal modulation. A possible choice for orthogonal symbols is the application of the well-known Walsh-functions as suggested in [2]. Channel encoding and symbol mapping (modulation) result in a spectral spreading factor of $M/(R \cdot \log_2(M))$. Further spreading by a factor of N_p is carried out by multiplication with a

[2] In this paper signals are described in vector representation, i.e. the samples of the finite length symbol $h_j(kT_c)$ are collected in a vector $\boldsymbol{h}_j = [h_j(0), h_j(T_c), \ldots, h_j((N-1)T_c]^T$.

user-specific pseudo noise sequence ("pn code"). If this code is designed as a complex sequence, so called "quadrature spreading" is introduced which allows the application of *Offset-QPSK* in order to minimise the effects of nonlinear amplifier distortions caused by large amplitude variations. Channel encoding, modulation and pn-spreading result in an overall spectral spreading factor ("processing gain") of

$$P_G = N_p \cdot M/(R \cdot \log_2(M)) \ . \tag{1}$$

After radio transmission, a signal corrupted by additve white Gaussian noise and multipath propagation is obtained. Multipath correction can easily be accomplished by means of the well-known RAKE receiver [11]. After low-pass transformation and despreading we get the complex signal (in vector representation)

$$\boldsymbol{s}^{(\mu)} = c_\mu \boldsymbol{h}_i + \boldsymbol{r}^{(\mu)}, \qquad \mu \in \{0, \dots, L-1\} \tag{2}$$

on the μ-th RAKE-tap where c_μ denotes the (complex) magnitude of the μ-th channel echo and $\boldsymbol{r}^{(\mu)}$ represents the influence of the additive channel noise, multiple access interference (MAI) and RAKE-path interference in case of non-ideal orthogonality properties of the pn-code. The elements of $\boldsymbol{r}^{(\mu)}$ can be regarded as uncorrelated Gaussian stochastic variables with power σ_r^2 each.

For the symbol decision, this signal has to be correlated with each of the M symbols $\boldsymbol{h}_j$, $j = 0, \dots, M-1$, which can be solved efficiently by the fast Hadamard transform [12]. In order to obtain a *noncoherent* decision rule we calculate the squared magnitudes of the correlation results. Thus, we obtain a number of M decision variables at the μ-th RAKE-tap

$$V_j^{(\mu)} = |\boldsymbol{h}_j^T \boldsymbol{s}^{(\mu)}|^2 = |c_\mu E_h \delta_{ij} + \boldsymbol{h}_j^T \boldsymbol{r}^{(\mu)}|^2, \quad j \in \{0, \dots, M-1\} \tag{3}$$

with the Kronecker symbol δ_{ij} and the symbol energy $E_h = \boldsymbol{h}_j^T \boldsymbol{h}_j$. The term $\boldsymbol{h}_j^T \boldsymbol{r}^{(\mu)}$ represents a complex stochastic white process with variance $E_h \sigma_r^2$. Next, the M-dimensional vectors $\boldsymbol{V}^{(\mu)} = [V_0^{(\mu)}, \dots, V_{M-1}^{(\mu)}]^T$ from all RAKE-taps are summed up (*square-law combining*)

$$\boldsymbol{V} = \sum_{\mu=0}^{L-1} \boldsymbol{V}^{(\mu)}, \quad \boldsymbol{V} = [V_0, \dots, V_{M-1}]^T, \tag{4}$$

whereby the choice of the component with maximum magnitude leads to the symbol decision:

$$\max_{(j)} \{V_0, \dots, V_j, \dots, V_{M-1}\} \ \Rightarrow \ \hat{V}_i. \tag{5}$$

Finally, the transmitted binary data is obtained by symbol-to-bit mapping.

The well-known QUALCOMM-proposal recently defined as the IS-95 standard for cellular telephone transmission [4] is based on the CDMA scheme discussed above.

2.2 Soft Decision Channel Decoding in Noncoherent Receivers for M-ary Orthogonal Modulation

The optimum strategy for channel decoding is given through soft decision ML decoding, efficiently carried out using a Viterbi decoder. As explained, the noncoherent receiver for M-ary orthogonal modulation performs *hard symbol decisions* according to eq. (5). However, some form of soft reliability information about these decisions should be available serving as the input of the Viterbi decoder. It has been shown in [8] that these soft-decisions have to be supplied in a bit-specific manner to the decoder to achieve a minimum BER. In the following, a maximum likelihood (ML) criterion for noncoherent demodulation of M-ary orthogonally modulated signals will be derived as previously proposed in [9].

Let us first assume binary antipodal transmission with $b_\nu \in \{-1,+1\}$ denoting the ν-th transmitted encoded symbol. Hard decision at the receiver leads to the binary encoded symbol $z_\nu \in \{-1,+1\}$. If sufficient interleaving is applied, the inner channel consisting of the interleaver, modulator, mobile radio channel, demodulator, and deinterleaver can be modelled as a memoryless discrete binary symmetric channel characterised by the probability for correct decision $P_\nu := P(z_\nu = b_\nu)$. Consequently, for incorrect decision we get $P(z_\nu \neq b_\nu) = 1 - P_\nu$. In that case, the likelihood criterion for ML channel decoding is given by [15]

$$\Phi_{ML}^{BSC} = \sum_\nu b_\nu z_\nu \underbrace{\log \frac{P_\nu}{1-P_\nu}}_{=:\ L_\nu} \stackrel{!}{=} \max \ . \tag{6}$$

This can be solved efficiently by the Viterbi algorithm where $z_\nu \cdot \log \frac{P_\nu}{1-P_\nu} = z_\nu \cdot L_\nu$ serves as a soft input signal. In this context, L_ν can be interpreted as a reliability indicator for the hard decided code bit z_ν. If L_ν is constant in time, it can be factored out and thus does not influence the decoding process (6). If, however, L_ν changes with time index ν the application of eq. (6) results in optimum performance under time-variant channels (e.g. mobile radio transmission).

Let us now return to the problem of M-ary orthogonal modulation with noncoherent detection. As outlined in the previous section, we carry out hard symbol decisions after fast Hadamard transform where each symbol represents a group of $\log_2(M)$ bits. For optimum channel decoding, *bit-specific reliability information* is required.

Let us start with the calculation of the conditional probability that $\boldsymbol{h}_j$ is the transmitted symbol under the observation of $\boldsymbol{V}$. Applying the Bayes law results in

$$P(\boldsymbol{h}_j|\boldsymbol{V}) \ = \ \frac{P(\boldsymbol{h}_j)}{p(\boldsymbol{V})} \cdot p(\boldsymbol{V}|\boldsymbol{h}_j) \ . \tag{7}$$

If equiprobable transmitted symbols $\boldsymbol{h}_j$ are assumed, we get $P(\boldsymbol{h}_j) = 1/M$. Due to the statistical independence of the components of $\boldsymbol{V}$, the conditional probability density $p(\boldsymbol{V}|\boldsymbol{h}_j)$ can be written as a product

$$p(\boldsymbol{V}|\boldsymbol{h}_j) \;=\; q(V_0)\cdot q(V_1)\cdot\ldots\cdot Q(V_j)\cdot\ldots\cdot q(V_{M-1}) \tag{8}$$

where $q(V_k) = p(V_k|\boldsymbol{h}_j \neq \boldsymbol{h}_k)$ and $Q(V_j) = p(V_j|\boldsymbol{h}_j)$. The terms $q(V_k)$ and $Q(V_j)$ can be calculated uniquely. Let the noncoherent RAKE receiver consist of L paths. Then L squared real and L squared imaginary parts of the decision variables $V_k^{(\mu)}$ are combined. Consider the k-th component where the current hypothesis $\boldsymbol{h}_j$ does not hold, i.e. $k \neq j$, then we get a summation of $2L$ squared Gaussian zero-mean random variables. This results in a chi^2-distribution with $2L$ degrees of freedom [14]:

$$q(V_k) = \frac{1}{\sigma^{2L}(L-1)!}\; V_k^{L-1}\,\exp(-\frac{V_k}{\sigma^2}) \tag{9}$$

with $\sigma^2 = E_h \cdot \sigma_r^2$. In contrast, for the j-th component corresponding to the current hypothesis $\boldsymbol{h}_j$ we obtain a non-central chi^2-distribution

$$Q(V_j) = \frac{1}{\sigma^2}\left(\frac{V_j}{\rho^2}\right)^{\frac{L-1}{2}} \exp(-\frac{V_j+\rho^2}{\sigma^2})\cdot \mathrm{I}_{L-1}\left(\frac{\rho\sqrt{V_j}}{\sigma^2/2}\right) \tag{10}$$

where the non-centrality is $\rho^2 = \sum_{\mu=0}^{L-1}(E_h|c_\mu|)^2$ and $\mathrm{I}_{L-1}(\cdot)$ denotes the modified Bessel function of order $L-1$.

With this, eq. (7) can be rewritten in the form

$$P(\boldsymbol{h}_j|\boldsymbol{V}) = \underbrace{\frac{1/M}{p(\boldsymbol{V})}\prod_{k=0}^{M-1} q(V_k)}_{=:\,\alpha}\cdot\frac{Q(V_j)}{q(V_j)}, \qquad j\in\{0,\ldots,M-1\}\,. \tag{11}$$

The unknown factor α can be determined indirectly by the exploitation of the relationship

$$\sum_{j=0}^{M-1} P(\boldsymbol{h}_j|\boldsymbol{V}) = \alpha\cdot\sum_{j=0}^{M-1}\frac{Q(V_j)}{q(V_j)} = 1 \tag{12}$$

(the union of all elementary events has probability one). The calculation of

$$\frac{Q(V_j)}{q(V_j)} = (L-1)!\cdot\frac{\sigma^{2(L-1)}}{\rho^{L-1}}\cdot\frac{\mathrm{I}_{L-1}\,(2\rho\sqrt{V_j}/\sigma^2)}{\exp(\rho^2/\sigma^2)\cdot V_j^{(L-1)/2}} \tag{13}$$

requires the knowledge of

$$\sigma^2 = \mathrm{E}\{|\boldsymbol{h}_j^T\boldsymbol{r}^{(\mu)}|^2\} \quad\text{and}\quad \rho^2 = E_h^2\sum_{\mu=0}^{L-1}|c_\mu|^2\;,$$

which are channel energy and noise power. These parameters can be estimated as follows:

(i) *noise power estimation*

If the hypothesis $\boldsymbol{h}_j$ is not true, the decision variables are determined by

$$V_j = \sum_{\mu=0}^{L-1} |\boldsymbol{h}_j^T \boldsymbol{r}^{(\mu)}|^2, \qquad j \neq i \ . \tag{14}$$

If we assume that the decision variable with maximum magnitude V_i represents the true hypothesis, we obviously get an estimate of the noise power $\hat{\sigma}^2$ by averaging over $M-1$ components of $V_j,\ j \neq i$, containing the false hypotheses:

$$\hat{\sigma}^2 = \frac{1}{M-1} \cdot \frac{1}{L} \sum_{\substack{j=0 \\ j\neq i}}^{M-1} V_j \ . \tag{15}$$

This estimation can be further improved by additional averaging in time direction.

(ii) *channel energy estimation*

In case of the true hypothesis $\boldsymbol{h}_j = \boldsymbol{h}_i$, the vector element $\boldsymbol{V}_i$ becomes

$$V_i = \sum_{\mu=0}^{L-1} |c_\mu E_h + \boldsymbol{h}_i^T \boldsymbol{r}^{(\mu)}|^2 = \underbrace{\sum_{\mu=0}^{L-1} |c_\mu|^2 E_h^2}_{\rho^2} + 2 \sum_{\mu=0}^{L-1} \mathrm{Re}\{c_\mu E_h \boldsymbol{h}_i^T \boldsymbol{r}^{(\mu)}\} + \sum_{\mu=0}^{L-1} |\boldsymbol{h}_i \boldsymbol{r}^{(\mu)}|^2 \ . \tag{16}$$

The second term on the right-hand side of (16) represents a Gaussian zero-mean stochastic variable which can be suppressed by time averaging. The bias caused by the third term on the right-hand side of (16) can be reduced by a correction term based on the noise estimation. Let k_0 be the current time index of the received Walsh-symbol. Then we get an appropriate estimation for the channel energy provided that the channel does not vary significantly within the time interval $k_0 - \Delta k + 1 \leq k \leq k_0$ by means of

$$\hat{\rho}^2 \approx \frac{1}{\Delta k} \cdot \sum_{k=k_0-\Delta k+1}^{k_0} V_i(k) - \underbrace{\frac{1}{\Delta k} \cdot \sum_{k=k_0-\Delta k+1}^{k_0} \sum_{\mu=0}^{L-1} |\boldsymbol{h}_i \boldsymbol{r}^{(\mu)}|^2}_{\approx L \cdot \hat{\sigma}^2} \ , \tag{17}$$

where the noise power $\hat{\sigma}^2$ estimated according to eq. (15) can be used here.

Taking into account the above considerations, all parameters needed for the calculation of the conditional symbol probability (11) are known. The results can be summarised for all M hypotheses: If the symbols $\boldsymbol{h}_j$ are replaced by their corresponding bit patterns

$\{b_0, \dots, b_{\log_2(M)-1}\}$ in antipodal representation, we get (illustrated for the case $M = 64$)

$$\begin{aligned} P(-1,-1,-1,-1,-1,-1|\boldsymbol{V}) &= \alpha \cdot Q(V_0)/q(V_0) \\ P(-1,-1,-1,-1,-1,+1|\boldsymbol{V}) &= \alpha \cdot Q(V_1)/q(V_1) \\ &\vdots \\ P(+1,+1,+1,+1,+1,+1|\boldsymbol{V}) &= \alpha \cdot Q(V_{M-1})/q(V_{M-1}). \end{aligned} \tag{18}$$

The application of eq. (6) requires knowledge of the probabilities of individual bit-decisions which can be gained by a columnwise evaluation of (18). Note, at first, that eq. (6) does not depend on the specific choice of the decision for bit z_ν, since

$$\begin{aligned} z_\nu = +1 \;\rightarrow\; z_\nu \cdot L_\nu &= +\log \frac{P(b_\nu = +1|\boldsymbol{V})}{1 - P(b_\nu = +1|\boldsymbol{V})} \qquad \text{and} \\ z_\nu = -1 \;\rightarrow\; z_\nu \cdot L_\nu &= -\log \frac{P(b_\nu = -1|\boldsymbol{V})}{1 - P(b_\nu = -1|\boldsymbol{V})} = \log \frac{1 - P(b_\nu = -1|\boldsymbol{V})}{P(b_\nu = -1|\boldsymbol{V})} \\ &= \log \frac{P(b_\nu = +1|\boldsymbol{V})}{1 - P(b_\nu = +1|\boldsymbol{V})} \end{aligned} \tag{19}$$

yield the same expression.

Now consider the calculation of soft information, e.g. for the first bit b_0 of the $\log_2(M)$-bit groups (most left bit-"column" in (18)): Adding all probabilities belonging to '$b_0 = 1$' we get

$$P(b_0 = 1|\boldsymbol{V}) = \sum_{M/2}^{M-1} P(\boldsymbol{h}_j|\boldsymbol{V}).$$

This leads to the reliability information for the first bit of the Walsh symbol being '$b_0 = 1$'

$$L_{b_0} = \log \frac{P(b_0 = 1|\boldsymbol{V})}{1 - P(b_0 = 1|\boldsymbol{V})}$$

and serves as a soft input for the Viterbi channel decoder. The other bits $b_1 \dots b_{\log_2(M)-1}$ are treated equivalently. Note that no explicit symbol decisions are carried out. Instead we get *individual reliability information* for each of the $\log_2(M)$ bits. This is an important difference to [2] where after symbol decision a reliability information is calculated which is common for all $\log_2(M)$ bits.

As a conclusion, a comparison of the ML-soft-decision criterion and the non bit-specific criterion according to [2] is given under the specific conditions of the QUALCOMM system. **Fig. 2** shows simulated BERs in presence of a "bad urban" channel. The gain of the QUALCOMM soft decision method is about 1.0 dB compared to hard decisions. The ML method results in an additional gain of 0.4 dB at BER $\approx 10^{-3}$. The dashed line demonstrates that a 3-bit quantisation

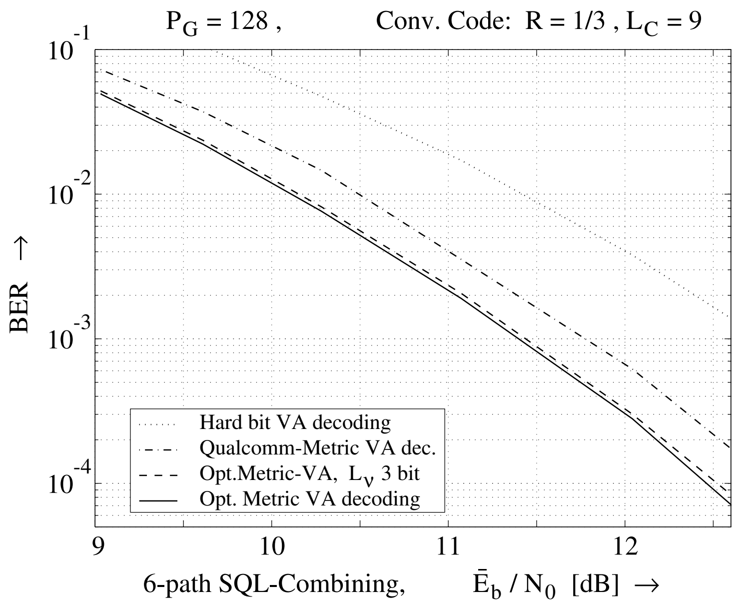

Fig. 2: Bit error rate for the QUALCOMM system with soft convolutional decoding (bad urban channel, mobile speed 60 km/h, carrier frequency 900 MHz).

of the soft input causes a slight degradation only. Further simulations not shown here exhibit that the ML method is robust to inaccurate estimation of the required channel state information according to eq. (15) and (17), respectively.

An alternative method recently published in [13], which also exploits bitwise reliability information is not shown in the figure. It is based on the same idea presented above but just uses two maximum decisions per bit instead of the whole M-ary vector. In addition, no channel state information is required. These modifications lead to an only slightly increased BER compared to the ML metric proposed in this paper. Therefore, the metric in [13] can be seen as an approach offering lower computational complexity with a performance quite close to the optimum ML metric.

3 System Design for Data Transmission

For the specific CDMA-system described in section 2.1, the QUALCOMM system, the parameter set $R = 1/3$ (code rate), $M = 64$ (M-ary Walsh modulation) and $N_p = 4$ (direct spreading) is chosen. According to eq. (1), this leads to a processing gain of $P_G = 128$. Now, we will vary these parameters keeping the processing gain unchanged. It is well known, that in AWGN channels the bit error rate continuously decreases with decreasing code rate R in the case of coherent detection. If noncoherent detection of M-ary orthogonal modulation is addressed, the bounds derived in [14] show that code rates in the vicinity of $1/2$ perform best. However, transmission over multipath fading channels requires interleaving, power control and – if necessary – a reasonably fast channel estimation. These practical requirements considerably influence system behaviour. It is shown for binary modulation techniques that code rates in the range of $1/4 \ldots 1/8$ perform best [16]. The investigations in [10] suggest that code rates $1/2 \ldots 1/3$ are the best choice applying the 64-ary noncoherent transmission scheme considered in section 2.1. If the 64-ary modulation is interpreted as a (64,6) block encoding, one may ask whether there is an optimum code rate, too, just as for convolutional encoding. In the general case, the bandwidth expansion by $M/\log_2(M)$ caused by the M-ary Walsh encoding has to be balanced against the expansion by $1/R$ due to convolutional encoding to achieve an optimum overall performance.

On account of the results published in [10], we confine our investigations to code rates not below $1/4$. For convenience, the polynomial representations of the convolutional codes used in this section are given in **Table 1**.

code rate	generators in octal	d_{free}
1/2	561 753	12
1/3	557 663 711	18
1/4	463 535 733 745	24

Table 1: Maximum free distance convolutional codes with constraint length $L_C = 9$ [14].

When transmitting convolutionally encoded data over fading channels, it is inevitable to perform sufficient interleaving because the Viterbi decoder at the receiver end is sensitive to burst errors. Since there is a restricted round-trip delay acceptable for e.g. speech traffic channels, only a limited number of information bits can be grouped for each interleaving block. With block interleaving, the number of rows (I) and columns (J) should be ([3])

$$I \geq \frac{1}{2 \cdot f_{D,max} \cdot T_R} = \frac{1}{2 \cdot f_{D,max} \cdot R \cdot T_b} \tag{20}$$

$$J \geq \frac{L_C}{R} \tag{21}$$

with $f_{D,max}$ denoting the maximum Doppler shift, $T_R = R \cdot T_b$ denoting the symbol period of the coded bits and L_C representing the constraint length of the convolutional code. Using the

[3] reading in per row and writing out per column at the interleaver (and vice versa at the deinterleaver)

rules given in eq. (20) and (21), it is obvious that the *interleaving delay* $T_{I/D}$ depends on the code rate R since

$$T_{I/D} \;=\; (I \cdot J) \cdot T_R \;=\; \left(\frac{1}{2 \cdot f_{D,max} \cdot T_R} \cdot \frac{L_C}{R} \right) \cdot T_R \;=\; \frac{L_C}{2 \cdot f_{D,max}} \cdot \frac{1}{R} \;\propto\; \frac{1}{R}\,. \tag{22}$$

Hence, an adequately dimensioned interleaver causes a longer delay the lower the code rate R is. On the other hand, given a *fixed interleaving delay* that is tolerable for a considered application, the process of *interleaving performs the better the higher the code rate is.* The latter statement especially holds if the interleaver is dimensioned quite scarce for a certain scenario, i.e. at relatively low Doppler shifts. In that case, the number of rows I according to eq. (20) may be too small which is further aggravated by a low code rate. This fact is illustrated in **Fig. 3**, where we assumed a multipath Rayleigh fading channel with four echoes for transmission as a typical mobile radio channel. The upper two groups of curves are obtained from simulations using different interleavers all with the same interleaving delay:

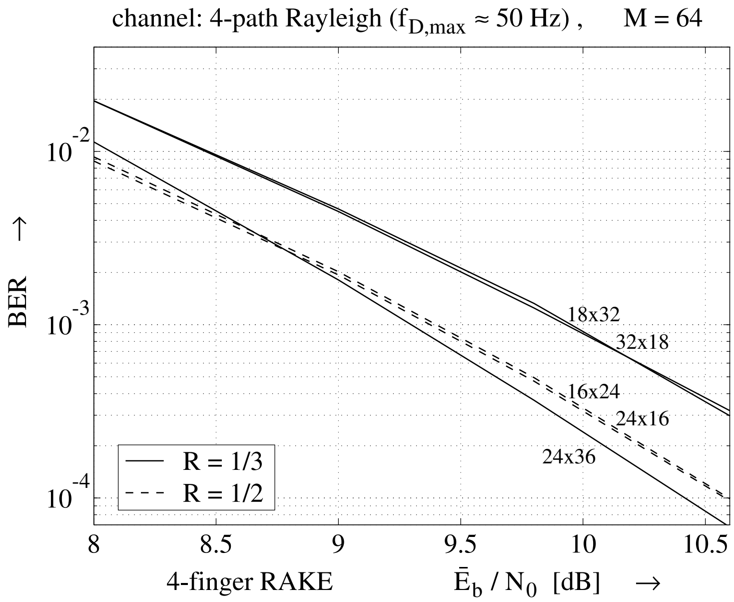

Fig. 3: Influence of interleaving for code rates $R = 1/3$ ($M = 64$, $N_p = 4$) and $R = 1/2$ ($M = 64$, $N_p = 6$) $\Rightarrow P_G = 128$ in all cases; carrier frequency 900 MHz, no power control.

$$\begin{aligned} T_{I/D} \;=\; (I \cdot J) \cdot T_R \;&=\; (18 \cdot 32) \cdot \frac{1}{3} \cdot T_b \;=\; (32 \cdot 18) \cdot \frac{1}{3} \cdot T_b \\ &=\; (16 \cdot 24) \cdot \frac{1}{2} \cdot T_b \;=\; (24 \cdot 16) \cdot \frac{1}{2} \cdot T_b \;=\; 20\,\text{ms} \;=\; \text{const.}\,. \end{aligned}$$

It can be seen that the system using the $R = 1/2$ coder outperforms the $R = 1/3$ system by ≈ 0.5 dB for all choices of I and J indicated above. If we do not assume a fixed delay and instead scale the interleaver in the case of $R=1/3$ proportionally to the dimensions used for $R=1/2$, i.e. multiply both the number of rows and number of columns by $\frac{1/2}{1/3} = 3/2$, we obtain nearly the same performance in both cases (see lower curve in Fig. 3: $I \times J = (16 \times 24) \cdot 3/2 = 24 \times 36$ for $R=1/3$). This, of course, would raise the interleaving delay to 30 ms.

The superiority of the interleaving for the coder with rate 1/2 to the 1/3 coder depends on the maximum Doppler shift $f_{D,max}$, as can be seen from eq. (20). Rearranging that inequality and using QUALCOMM's parameter set ($R = 1/3, I = 18$), it can be calculated that the mobile user's velocity would have to exceed

$$v \geq \frac{c}{f_0} \cdot \frac{1}{2 \cdot I \cdot R \cdot T_b} = 960\,\mathrm{km/h} \tag{23}$$

to enable the interleaver to sufficiently break deep fades, which is an unrealistic high value. For that, the 1/2 coder performs better for all velocities of practical interest in case of the 4-path Rayleigh channel under investigation, which is shown in **Fig. 4**. In all three cases the rate 1/2 coder performs better than the 1/3 coder. However, the gain in $\bar{E}_b/N_0$ decreases from 0.7 dB at $v = 15$ km/h to 0.4 dB at $v = 240$ km/h. Furthermore, in both cases $R = 1/2$ and $R = 1/3$, the interleaving performance improves as the fading becomes faster.

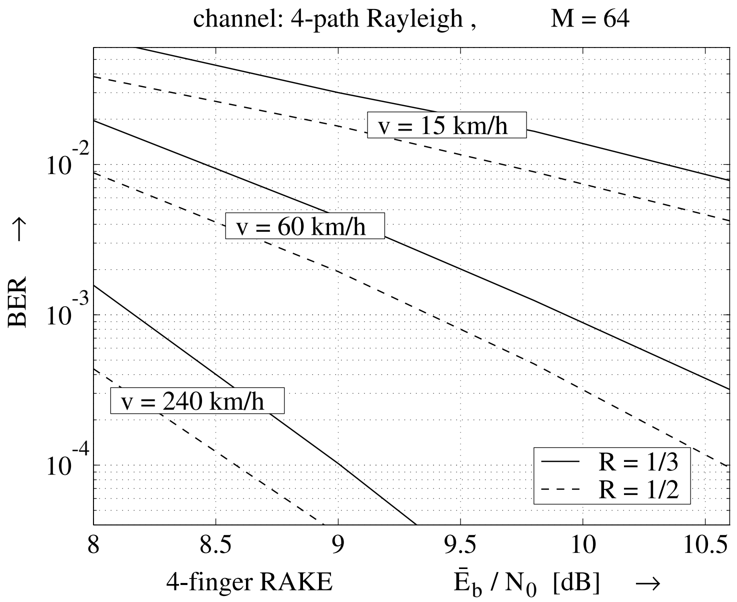

Fig. 4: Dependency of BER on code rate R and Doppler bandwidth for $f_{D,max} = 12.5, 50$ and 200 Hz corresponding to $v = 15, 60$ and 240 km/h, respectively ($P_G = 128$, carrier frequency 900 MHz, $T_{I/D} = 20$ ms = const., no power control).

Please note that in the simulation results shown here, tracking of the RAKE fingers is neglected for simplicity. Although tracking becomes more difficult with increasing velocity and thus is contrary to the effect of interleaving, we assume that tracking is feasible sufficiently accurate for the velocities under investigation.

Further results obtained from simulations at a constant processing gain of 128 and a fixed interleaving delay of 20 ms are shown in **Fig. 5**. As already deduced from Figs. 3 and 4, BER

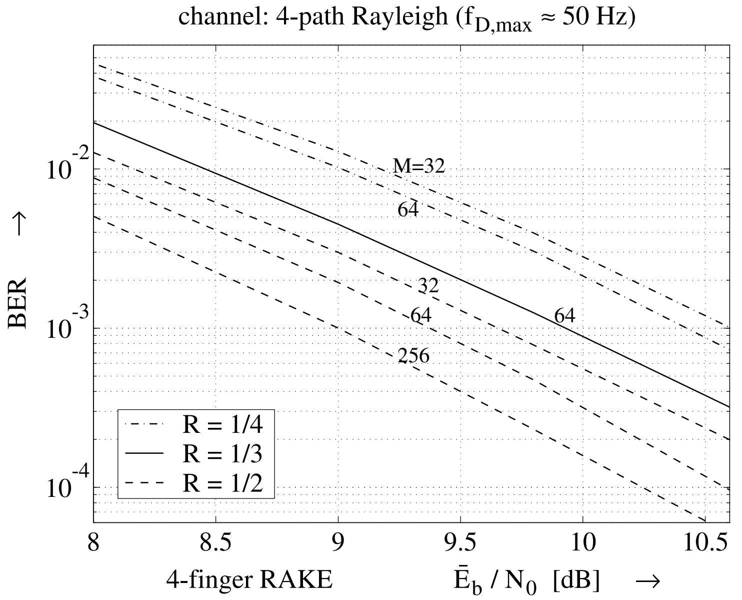

Fig. 5: Trade-off between code rate R, parameter M of Walsh modulation and remaining direct spreading at a fixed processing gain of $P_G = 128$ (carrier frequency 900 MHz, $T_{I/D} = 20\,\text{ms} = \text{const.}$, no power control).

decreases with increasing code rate. In addition, BER is lowered at a constant code rate due to a higher dimension of Walsh modulation. For example, for $R = 1/2$ we obtain a gain in terms of $\bar{E}_b/N_0$ of about 0.4 dB using $M = 256$ instead of $M = 64$. Comparing the QUALCOMM system (solid line) with the best case obtained here, the QUALCOMM-parameter choice leads to a loss of nearly 1.0 dB. Taking into account the complexity of both schemes, the one using $R = 1/2$ is superior in terms of convolutional encoding/decoding complexity. In contrast, the number of operations necessary for the M-ary Walsh demodulation using the fast Hadamard transform shows an opposite tendency being in the order of $\mathcal{O}(M\ \log_2(M))$ and therefore raises with increasing M. It should be further noted that a larger M effectively shortens the coherent integration time in the chip tracking loop (e.g. factor of direct spreading $N_p = 6$ (chips) in case of $M = 64$ compared to $N_p = 2$ in case of $M = 256$ with $R = 1/2$). However, since we assumed ideal tracking in our simulations, this impact is not included in the results.

The investigations lead to the following conclusions:

- Considering a constant interleaving delay and Doppler shifts of practical interest, it turns out that interleaving performs the better the *higher* the code rate R is.
- As much as possible of the remaining bandwidth expansion available after convolutional encoding should be exploited by Walsh modulation instead of "simple" spreading. The remaining bandwidth expansion increases with increasing code rate (i.e. "weaker coding"), too.
- The achievable gain compared to the QUALCOMM system ($R=1/3$, $M=64$, $N_p=4$) is in the order of 1.0 dB for the 4-path Rayleigh fading channel under investigation with the parameter set $R=1/2$, $M=256$ and $N_p=2$ (processing gain of 128 in both cases). Note that the simulations carried out for Fig. 5 were performed using the optimum soft metric for Viterbi decoding described in section 2.2 in all cases. For this reason, the gain would even raise to 1.3 dB when the original (suboptimum) metric is applied to the QUALCOMM system.

4 System Design for Video Transmission

Audio and video sequences generated through a parametric source coding process exhibit unequal sensitivity to transmission errors instead of equal error sensitivity as in the case of raw data. In the sequel we follow the error control strategy presented in [18] for optimum transmission of low data rate video in a mobile environment, which involves the application of unequal error protection by means of rate-compatible punctured convolutional codes (RCPC codes) [19] with one encoder in conjunction with soft decision maximum likelihood (ML) decoding through the Viterbi algorithm. For this, the ML metric derived in section 2.2 is applied for channel decoding. In contrast to the sharp interleaving delay restriction to 20 ms in section 3, convolutional interleaving over one image (video frame) is applied throughout the section. In case of a typical frame rate of $f_F = 5$ Hz, this results in an interleaving delay of $T_{I/D} = 200$ ms.
It must be emphasised that any augmented VA with soft output may be applied for the provision of post-decoding reliability information, which allows efficient error concealment techniques to be applied for additional enhancement of the transmission quality as demonstrated in [20].

Fig. 6 depicts the post-decoding average BER as a function of the channel SNR ([4]) for the individual codes of the considered RCPC code family (mother code: code rate=1/3, memory=6,

[4] Note that in contrast to Figs. 4 and 5, where the BER is a function of $\bar{E}_b/N_0$, here, it is a function of $\bar{E}_S/N_0$. However, it is the proper representation for the case considered here.

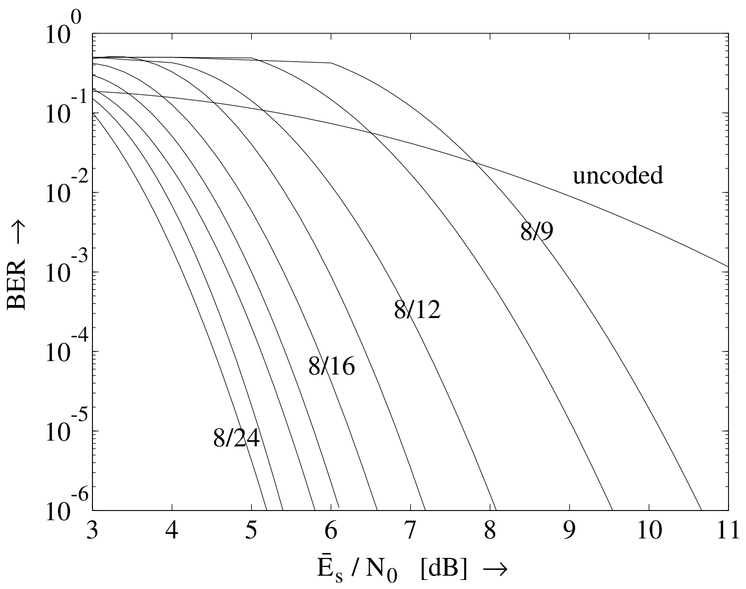

Fig. 6: Performance (simulation) of the RCPC code family for coded DS-CDMA and partially interleaved BU channel (carrier frequency 2 GHz, $f_{D,max} = 200$ Hz).

puncturing period=8) with soft decision ML decoding obtained through simulation of the point-to-point DS-CDMA-based transmission link.

A p×8 kbit/s, p=1,...,8, hybrid video source coding scheme, much like the H.261 ISDN standard, characterised by QCIF spatial resolution and a temporal resolution (frame rate) $f_F \leq 10$ Hz is applied for wireless videotelephony in the considered DS-CDMA-based system (refer to section 2) in the sequel. Due to the underlying parametric encoding process, the j-th image is represented by parameter sets of variable length $n_k^{(j)}, k = 1, \ldots, 7$, with different information contents such as contour (CT), motion vectors (MV), block location (BI), discrete cosine transform coefficients (DCT), quantiser levels (QL), quadtree (QT) and structure indices (SI). The sensitivity of the individual parameter sets (source classes) to transmission errors can be acquired by considering as an objective measure the source post-decoding average noise power due to independent single bit transmission errors as in [18]

$$10 \log_{10}(A_k) = \frac{1}{J} \sum_{j=1}^{J} 10 \log_{10} \left(\frac{1}{n_k^{(j)}} \sum_{i=1}^{n_k^{(j)}} \frac{||\boldsymbol{u}^{(j)} - \hat{\boldsymbol{u}}_i^{(j)}||^2 - ||\boldsymbol{u}^{(j)} - \hat{\boldsymbol{u}}^{(j)}||^2}{||\boldsymbol{u}^{(j)}||^2} \right) \tag{24}$$

represented by the sensitivity coefficients $A_k, k = 1, \ldots, 7$. Here $\boldsymbol{u}^{(j)}$ denotes the original image, $\hat{\boldsymbol{u}}^{(j)}$ the reconstructed image in the case of an error free transmission and $\hat{\boldsymbol{u}}_i^{(j)}$ the reconstructed image in the case of an error in bit position i of the j-th image. Then, the individual code rates R_k are chosen in such a way that after error protection each parameter set (sensitivity class) contributes the same to the overall average noise caused by transmission errors. **Table 2** summarises the obtained sensitivity coefficients of the applied video codec and the allocated redundancy per parameter set in the case of the video test sequence “Miss America” and a net source data rate $R_v = 16$ kbit/s.

Source class k	Error sensitivity $-10\ \log_{10}(A_k)$ [dB]	Code rate R_k
1: CT	16.29	8/18
2: MV	13.95	8/18
3: BI	18.57	8/18
4: DCT	22.75	8/16
5: QL	24.08	8/16
6: QT	29.20	8/16
7: SI	44.09	8/14

Table 2: Source error sensitivity and unequal error protection (“Miss America”, QCIF with $p = 2$, $f_F = 5$ Hz, mean code rate $R = 1/2$).

The system optimisation involves the optimum choice of key parameters such as source accuracy (net mean source data rate R_v), redundancy (mean code rate R) and spectral spreading factor $S_F = P_G \cdot R$ under consideration of the selective error protection addressed above. Although an adaptive approach could be used, we consider an optimisation strategy in discrete steps, i.e. the system performance is assessed for a finite number of values of the set $\{R_v, R, S_F\}$ through simulation, from which the optimum parameters can be identified. This is accomplished for both subsets $\{R_v, R\}$ and $\{R, S_F\}$ independently, whereby the segmental SNR

$$\text{SEGSNR} = \frac{1}{J}\sum_{j=1}^{J} 10\ \log_{10} \frac{||\boldsymbol{u}^{(j)}||^2}{||\boldsymbol{u}^{(j)} - \hat{\boldsymbol{u}}_i^{(j)}||^2} \tag{25}$$

known from the speech processing field is applied as an objective performance criterion in the case of the underlying video transmission. Furthermore, we consider three different system operating points characterised by a channel signal to noise ratio $\text{SNR}_c = 10\log_{10}(E_S/N_0) = 10.3, 7.3$ and 5.5 dB which corresponds to 3,6 and 9 users respectively. Note that the SNR_c characterises the total additive interference, i.e. thermal noise (AWGN) plus multiple users within a cell (MAI). The gross average information data rate is fixed to $R_v/R = 32$ kbit/s, while the transmitted signal is characterised by a data rate $S_F R_v/R = 1.024$ MChip/s throughout the section.

The choice of the set $\{R_v, R\}$ represents a trade-off between source accuracy and error protection for a constant gross information data rate $R_v/R = 32$ kbit/s. With this respect,

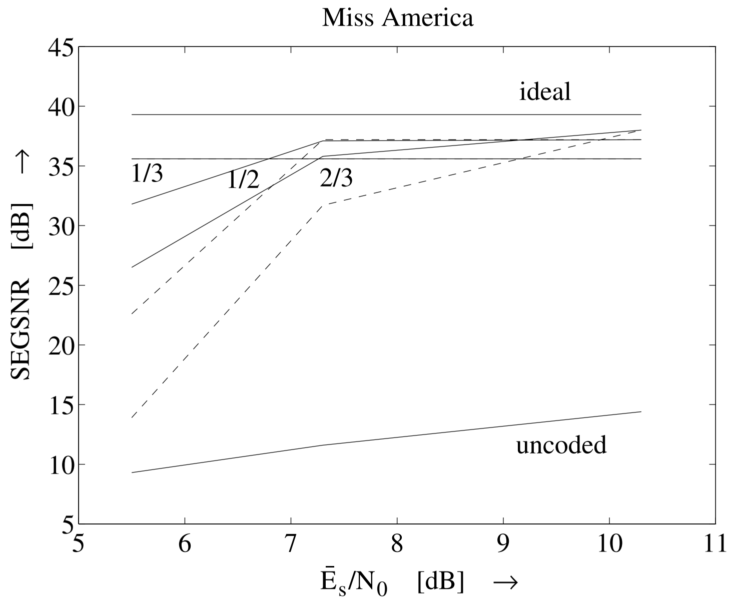

Fig. 7: Trade-off between source accuracy (R_v) and error protection (R) in the case of unequal (-) and equal (- -) error protection. Note that in the case of $R = 1/3$ both SEGSNRs are equivalent.

Fig. 7 depicts the resulting system performance characterised by the SEGSNR at the video codec output in the case of unequal (-) and equal (- -) error protection. First, the gain due to unequal error protection for low SNRs implies a higher system capacity regarding the total number of users which the system can support within a cell for a specific transmission quality. Secondly, a mean code rate $R = 1/2$ represents a good compromise for the range of SNRs considered.

Analogous to the above considerations the choice of the set $\{R, S_F\}$ represents a trade-off between error protection and spectral spreading for a constant processing gain $P_G = S_F/R = 64$. **Fig. 8** reveals that the spreading factor should be chosen as high as possible in conjunction with a moderate code rate. Note that the variation of S_F has been achieved through variation of the spreading factor of the first stage, i.e. the modulation order. Since signal spreading can be interpreted as a channel coding process, the underlying system represents a concatenated code consisting of an inner nonbinary block code and an outer binary convolutional code. Due to the partial interleaving applied, convolutional decoding will be optimum in the case of random errors at the decoder input, which can be achieved by increasing the error correction capability of the inner block code.

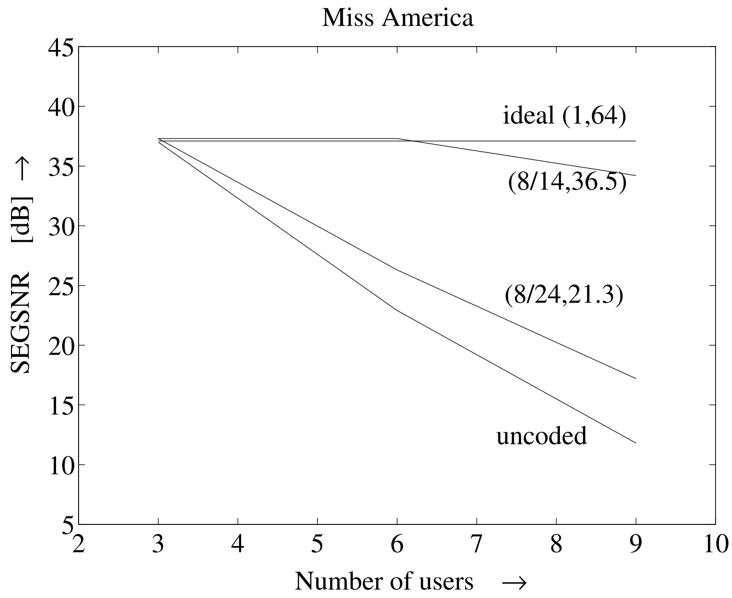

Fig. 8: Trade-off between error protection R and spectral spreading S_F (set (R, S_F) in the legend).

5 Conclusions

In this paper, an optimisation of the transmission quality in the noncoherent uplink of a DS-CDMA-based mobile communication system for data (speech) and video services has been presented. This includes a technique for the generation of post-decision reliability information in the case of a noncoherent RAKE receiver. The scheme avoids hard symbol decisions in the inner demodulation procedure and supplies the outer decoder with *bitwise* instead of symbolwise soft information. With this, the ML decoding of the outer convolutional code leads to a gain of nearly 0.5 dB compared to the BER performance of the well-known QUALCOMM system.

For both data and video transmission, a compound design instead of an independent design of individual techniques (e.g. source coding, channel coding, modulation, spectral spreading) is carried out, which results in optimum performance. It is shown for data transmission that the restricted interleaving delay leads to remarkably high code rates to be considered in a practical design, e.g. $R = 1/2$. The optimisation finally leads to a gain of more than 1.0 dB with a negligible increase of system complexity. For video transmission, key parameters for unequal error protection are chosen according to a discrete optimisation procedure through simulation of the point-to-point transmission link. A *mean* code rate $R = 1/2$ represents a good compromise for the range of SNRs considered, while a large spreading factor in connection with a moderate mean code rate and a fixed processing gain yields optimum results. Since spectral spreading can be interpreted as a block coding process, unequal spreading represents an interesting topic for further research in line with the followed matched error control strategy.

Acknowledgement

The authors would like to express their thanks to the anonymus reviewers for their helpful comments and suggestions.

References

[1] A. Salmasi and K. Gilhousen: *On the System Design Aspects of Code Division Multiple Access (CDMA) Applied to Digital Cellular and Personal Communication Networks*, Proc. IEEE Vehicular Technology, pp. 57-62, St. Louis, May 1991.

[2] A.J. Viterbi, A.M. Viterbi, and E. Zehavi: *Performance of Power-Controlled Wideband Terrestrical Digital Communication*, IEEE Trans. on Communications, Vol. 41, pp. 559-569, April 1993.

[3] A.J. Viterbi: *The Orthogonal Random Waveform Dichotomy for Digital Mobile Personal Communications*, IEEE Personal Communications, Vol. 1, No. 1, pp. 18-24, 1994.

[4] TIA/EIA Interim Standard IS-95: *Mobile Station – Base Station Compatibility Standard for Dual-Mode Wideband Spread Spectrum Cellular System*, Telecommunications Industry Association, July 1993.

[5] A. Baier: *An open Multi-Rate Radio Interface Based on DS-CDMA – The Radio Interface Concept of CODIT*, Proc. RACE Mobile Telecommunication Workshop, pp. 123-128, Metz, June 1993.

[6] M. Benthin: *Vergleich kohärenter und inkohärenter Codemultiplex-Übertragungskonzepte für zellulare Mobilfunksysteme*, VDI-Verlag, Reihe 10: Informatik/Kommunikationstechnik, No. 424, Düsseldorf, 1996.

[7] J. Hagenauer: *Viterbi Decoding of Convolutional Codes for Fading and Burst Channels*, Proc. of the 1980 Zurich Seminar on Digital Communications, IEEE Cat. No. 80CH1521-4, pp. G2.1-G2.7, 1980.

[8] E. Zehavi: *8-PSK Trellis Codes for a Rayleigh Channel*, IEEE Trans. on Communications, Vol. 40, No. 5, pp. 873-884, May 1992.

[9] M. Benthin and K.D. Kammeyer: *Viterbi Decoding of Convolutional Codes With Reliability Information for a Noncoherent RAKE-Receiver in a CDMA-Environment*, IEEE GLOBECOM '94, San Francisco, Nov. 1994.

[10] M. Bickel, W. Granzow, and P. Schramm: *Optimization of Code Rate and Spreading Factor for Direct Sequence CDMA Systems*, Proc. IEEE Fourth Int. Symposium on Spread Spectrum Techniques and Applications (ISSSTA'96), Vol. 2, pp. 585-589, Mainz, Germany, Sept. 1996.

[11] K.D. Kammeyer: *Nachrichtenübertragung*, 2nd edition, B.G. Teubner, Stuttgart 1996.

[12] J. Borish and J.B. Angell: *An Efficient Algorithm for Measuring the Impulse Response Using Pseudorandom Noise*, Journal of the Audio Engineering Society, Vol. 31, No. 7, pp. 478-487, July/Aug. 1983.

[13] A.J. Viterbi: *CDMA – Principles of Spread Spectrum Communication*, Addison–Wesley, Reading 1995.

[14] J. Proakis: *Digital Communication*, 3rd edition, McGraw Hill, New York 1995.

[15] J. Hagenauer: *A Viterbi Algorithm with Soft-Decision Outputs and its Application*, Proc. GLOBECOM'89, Dallas, Texas, Vol. 3, pp. 1680-1686, 1989.

[16] P. Hoeher: *Unequal Error Protection for Digital Mobile DS-CDMA Systems*, Proc. IEEE Int. Conference on Communications (ICC'94), pp. 1236-1241, May 1994.

[17] R.V. Cox, J. Hagenauer, N. Seshadri, and C.-E. Sundberg: *Sub-Band Speech Coding and Matched Convolutional Channel Coding for Mobile Radio Channels*, IEEE Trans. On Signal Processing, Vol. ASSP-39, pp. 1717-1731, 1991.

[18] R. Mann Pelz: *An Unequal Error Protected $p \times 8$ kbit/s Video Transmission for DECT*, Proc. IEEE Vehicular Techn. Conference (VTC'94), pp. 1020-1024, Stockholm, 1994.

[19] J. Hagenauer: *Rate-Compatible Punctured Convolutional Codes (RCPC Codes) and their Applications*, IEEE Trans. on Communications, Vol. 36, No. 4, pp. 389-400, April 1988.

[20] R. Mann Pelz and J. Bechir: *Error Concealment for robust Arithmetic Decoding in Mobile Radio Environments*, Signal Processing: Image Communications, No. 8, pp. 411-419, 1996.